HOSTED BY

ELSEVIER

Available online at www.sciencedirect.com

ScienceDirect

Journal of Sport and Health Science 00 (2024) 1–11

Original article

The deterministic condition for the ground reaction force acting point on the combined knee valgus and tibial internal rotation moments in early phase of cutting maneuvers in female athletes

Issei Ogasawara [a,*], Ken Ohta [b], Gajanan S. Revankar [c], Shoji Konda [a], Yohei Shimokochi [d], Hideyuki Koga [e], Ken Nakata [a]

[a] *Department of Health and Sport Sciences, Graduate School of Medicine, Osaka University, Toyonaka 560-0043, Japan*
[b] *Sports Sensing Co., LTD., Fukuoka 815-0035, Japan*
[c] *Department of Neurology, Graduate School of Medicine, Osaka University, Suita 565-0871, Japan*
[d] *Department of Health and Sport Management, Osaka University of Health and Sport Sciences, Sennan-gun 590-0496, Japan*
[e] *Department of Joint Surgery and Sports Medicine, Graduate School of Medical and Dental Sciences, Tokyo Medical and Dental University, Bunkyo-ku 113-8519, Japan*

Received 25 January 2023; revised 15 September 2023; accepted 8 October 2023

Abstract

Background: Combined knee valgus and tibial internal rotation (VL + IR) moments have been shown to stress the anterior cruciate ligament (ACL) in several *in vitro* cadaveric studies. To utilize this knowledge for non-contact ACL injury prevention in sports, it is necessary to elucidate how the ground reaction force (GRF) acting point (center of pressure (CoP)) in the stance foot produces combined knee VL + IR moments in risky maneuvers, such as cuttings. However, the effects of the GRF acting point on the development of the combined knee VL + IR moment in cutting are still unknown.

Methods: We first established the deterministic mechanical condition that the CoP position relative to the tibial rotational axis differentiates the GRF vector's directional probability for developing the combined knee VL + IR moment, and theoretically predicted that when the CoP is posterior to the tibial rotational axis, the GRF vector is more likely to produce the combined knee VL + IR moment than when the CoP is anterior to the tibial rotational axis. Then, we tested a stochastic aspect of our theory in a lab-controlled *in vivo* experiment. Fourteen females performed 60° cutting under forefoot/rearfoot strike conditions (10 trials each). The positions of lower limb markers and GRF data were measured, and the knee moment due to GRF vector was calculated. The trials were divided into anterior- and posterior-CoP groups depending on the CoP position relative to the tibial rotational axis at each 10 ms interval from 0 to 100 ms after foot strike, and the occurrence rate of the combined knee VL + IR moment was compared between trial groups.

Results: The posterior-CoP group showed significantly higher occurrence rates of the combined knee VL + IR moment (maximum of 82.8%) at every time point than those of the anterior-CoP trials, as theoretically predicted by the deterministic mechanical condition.

Conclusion: The rearfoot strikes inducing the posterior CoP should be avoided to reduce the risk of non-contact ACL injury associated with the combined knee VL + IR stress.

Keywords: Center of pressure; Deterministic condition; Foot strike pattern; Injury mechanism; Moment of ground reaction force

1. Introduction

The anterior cruciate ligament (ACL) primarily restrains the tibial anterior translation relative to the femur in the sagittal plane.[1] The tibial anterior shear force due to isolated quadriceps contraction under shallow knee flexion angle[2,3] or other external forces, such as ski boot-induced anterior drawer,[4] directly adds to ACL stress. From its oblique orientation relative to the knee rotational axes, the ACL is also responsible for knee valgus stress in the frontal plane[5,6] as well as internal tibial rotational stress in the horizontal plane.[7] Injurious kinematics, such as dynamic valgus collapse and/or excessive tibial rotation, are typically seen in ACL injury situations in sports.[8–10] Although the ACL plays an essential

Peer review under responsibility of Shanghai University of Sport.
*Corresponding author.
E-mail address: ogasawaraissei@hss.osaka-u.ac.jp (I. Ogasawara).

https://doi.org/10.1016/j.jshs.2023.11.005

role for 3-dimensional (3D) knee stability for each plane, it is prone to a combination of multi-directional stresses during athletic maneuvers.[11,12] At the joint level, *in vitro* cadaveric studies have reported that combined knee valgus and tibial internal rotation (VL + IR) moments specifically increase stress on the ACL[13–16] and are therefore considered to be a primary mechanism in non-contact ACL injuries.[11,12] However, it is yet to be determined what kind of mechanical condition is behind the generation of combined knee VL + IR moments during complex sporting maneuvers.

Often, non-contact ACL injuries occur without any direct blow to the knee.[17,18] The ground reaction force (GRF) acting on the stance foot is a unique but significant external force that produces risky translational/rotational loadings on the knee. Prior studies suggest that inappropriate lines of action between the GRF vector and the shank segment produce at-risk knee loadings. For example, it has been suggested that the lateral GRF component relative to the shank segment is what applies the knee valgus moment in cutting maneuvers.[19–21] The anterior GRF component relative to the tibial rotational axis during landing with upright torso[22] or cutting with rearfoot strike[23] result in a tibial anterior shear force. Collectively, these *in vivo* controlled studies have empirically identified the task-specific GRF orientation that induces risky knee loadings. However, these studies were limited to single-plane loading, and to our knowledge, no studies have so far identified the deterministic role of the GRF acting point or the orientation of the GRF vector on the generation of the combined knee VL + IR moment.

Videographic studies have reported high ACL injury rates during sharp deceleration movements with heel strikes.[24,25] In contrast, the forefoot landing has been seen consistently in similar deceleration movements that did not result in ACL disruption.[26,27] The lab-controlled study by Ogasawara et al.[28] reported that rearfoot strikes were more likely than forefoot strikes to generate the combined knee VL + IR moment in cuttings. These contrasting clinical findings beg the question: Do different GRF acting points (center of pressure (CoP)) across tibial rotational axis in sagittal plane differentiate knee biomechanics and affect the likelihood of applying the combined knee VL + IR moment during deceleration maneuvers?

To unpack this question, we first utilized Euler's equation of motion to theoretically determine the mechanical condition that the CoP position relative to the tibial rotational axis differentiates the GRF vector's directional probability for the combined knee VL + IR moment development. Then, we tested a stochastic aspect of our theory in a lab-controlled experimental setting, hypothesizing that when the CoP is posterior to the tibial rotational axis, the GRF vector is more likely to produce the combined knee VL + IR moment than when the CoP is anterior to the tibial rotational axis. This hypothesis was based on the deterministic mechanical condition described below, which states that the GRF vector acting posterior to the tibial rotational axis has a greater directional probability of applying the combined knee VL + IR moment than the GRF vector acting anterior to the tibial rotational axis.

2. Methods

2.1. Theory of the deterministic condition for the combined knee VL + IR moment

2.1.1. Model

A 2-link lower limb model consisting of shank and foot segments of the right leg was defined (Fig. 1). The position vectors $\boldsymbol{x}_k$, $\boldsymbol{x}_a$, and $\boldsymbol{x}_c$ are pointing from the origin of global coordinate system (GCS) Σ^O to the knee joint center (KJC), ankle joint center, and CoP, respectively. The longitudinal axis of the shank segment, which is tibial rotational axis, is defined as a line connecting the ankle joint center and KJC. The vector $\boldsymbol{f}$ indicates the GRF vector applied to the foot. The varus/valgus rotational axis is defined as an anteriorly directing unit vector $\boldsymbol{e}_{\mathrm{v/v}}$ where the subscript v/v denotes varus/valgus. The tibial internal/external rotational axis is defined as a unit vector $\boldsymbol{e}_{\mathrm{i/e}}$, where the subscript i/e denotes internal/external. This vector is along the shank longitudinal axis and directs proximally. The extension/flexion axis is defined as a unit vector $\boldsymbol{e}_{\mathrm{e/f}}$ directing to the left side of the knee. These unit vectors were mutually orthogonal. The transformation matrix from the GCS Σ^O to the shank coordinate system (SCS) Σ^S is defined as $\boldsymbol{R}^S \equiv \left[\boldsymbol{e}_{\mathrm{v/v}} \quad \boldsymbol{e}_{\mathrm{e/f}} \quad \boldsymbol{e}_{\mathrm{i/e}}\right]$, where the superscript S denotes the SCS. The moment arm vector $\boldsymbol{r}_c$

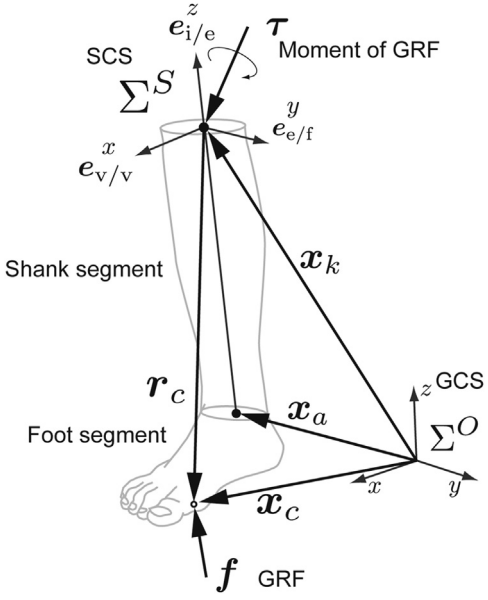

Fig. 1. A 2-link lower limb model consisting of the foot and shank segment expressed in the GCS Σ^O. The unit vector $\boldsymbol{e}_{\mathrm{v/v}}$ points anteriorly and corresponds to the varus/valgus rotation axis of the knee. The unit vector $\boldsymbol{e}_{\mathrm{i/e}}$, pointing proximally, represents the tibial internal/external rotation axis. The unit vector $\boldsymbol{e}_{\mathrm{e/f}}$, pointing leftward of leg, represents the knee extension/flexion axis. The unit vectors $\boldsymbol{e}_{\mathrm{v/v}}$, $\boldsymbol{e}_{\mathrm{e/f}}$, and $\boldsymbol{e}_{\mathrm{i/e}}$ correspond to x, y, and z axis of the SCS Σ^S. $\boldsymbol{x}_k$, $\boldsymbol{x}_a$, and $\boldsymbol{x}_c$ is position vector from the origin of GCS to the KJC, the AJC, and the CoP, respectively. The moment arm vector $\boldsymbol{r}_c$ is the position vector going from the KJC to the position of the CoP. The GRF vector $\boldsymbol{f}$ applies at the CoP of the foot. The moment vector $\boldsymbol{\tau}$ is the moment of GRF applied at the KJC. AJC = ankle joint center; CoP = center of pressure; GCS = global coordinate system; GRF = ground reaction force; KJC = knee joint center; SCS = shank coordinate system.

Please cite this article as: Issei Ogasawara et al., The deterministic condition for the ground reaction force acting point on the combined knee valgus and tibial internal rotation moments in early phase of cutting maneuvers in female athletes, Journal of Sport and Health Science (2024), https://doi.org/10.1016/j.jshs.2023.11.005

is defined as a position vector pointing from the KJC to the position of the CoP.

Here we consider the moment of GRF applied to the shank at the KJC to be calculated as

$$\tau = \boldsymbol{r}_c \times f. \quad \text{Eq. (1)}$$

According to Euler's equation of motion, the direction of the moment of GRF can be affected by the position of the CoP. The projection of the moment of GRF $\boldsymbol{\tau}$ onto rotational axes $\boldsymbol{e}_{\mathrm{v/v}}$ and $\boldsymbol{e}_{\mathrm{i/e}}$ yields the knee varus/valgus and internal/external moment components

$$\tau_{\mathrm{v/v}} = \boldsymbol{e}_{\mathrm{v/v}}^{T}\boldsymbol{\tau} \quad \text{Eq. (2)}$$

and

$$\tau_{\mathrm{i/e}} = \boldsymbol{e}_{\mathrm{i/e}}^{T}\boldsymbol{\tau} \quad \text{Eq. (3)}$$

where the superscript T means the vector transpose. In the right-side knee, the condition satisfying

$$\tau_{\mathrm{v/v}} < 0 \quad \text{Eq. (4)}$$

and

$$\tau_{\mathrm{i/e}} > 0 \quad \text{Eq. (5)}$$

indicates that the GRF vector causes the combined knee VL + IR moment and adds stress onto the ACL.[14,15]

2.1.2. *Effect of CoP position on the GRF vector's orientation range for applying the combined knee VL + IR moment*

Here, we show that the directional range of the GRF vector, which causes the combined knee VL + IR moment, becomes wider when the CoP is posterior to the tibial rotational axis. The 2 moving planes, $P_{\mathrm{v/v}}$ and $P_{\mathrm{i/e}}$, are introduced to separate 3D spaces, which define force directions causing each VL and IR moment (Fig. 2). $P_{\mathrm{v/v}}$ is the plane spanned by the varus/valgus rotational axis $\boldsymbol{e}_{\mathrm{v/v}}$ and the moment arm vector $\boldsymbol{r}_c$. $P_{\mathrm{i/e}}$ is the plane spanned by the internal/external rotation axis $\boldsymbol{e}_{\mathrm{i/e}}$ and $\boldsymbol{r}_c$. These 2 planes intersect the KJC and separate the 3D space into 2 regions: S^{+} and S^{-}. The superscripts + and − denote the positive and negative side of each plane, respectively. The unit normal vectors of those planes

$$\boldsymbol{n}_{\mathrm{v/v}} = \frac{\boldsymbol{e}_{\mathrm{v/v}} \times \boldsymbol{r}_c}{\| \boldsymbol{e}_{\mathrm{v/v}} \times \boldsymbol{r}_c \|} \quad \text{Eq. (6)}$$

and

$$\boldsymbol{n}_{\mathrm{i/e}} = \frac{\boldsymbol{e}_{\mathrm{i/e}} \times \boldsymbol{r}_c}{\| \boldsymbol{e}_{\mathrm{i/e}} \times \boldsymbol{r}_c \|} \quad \text{Eq. (7)}$$

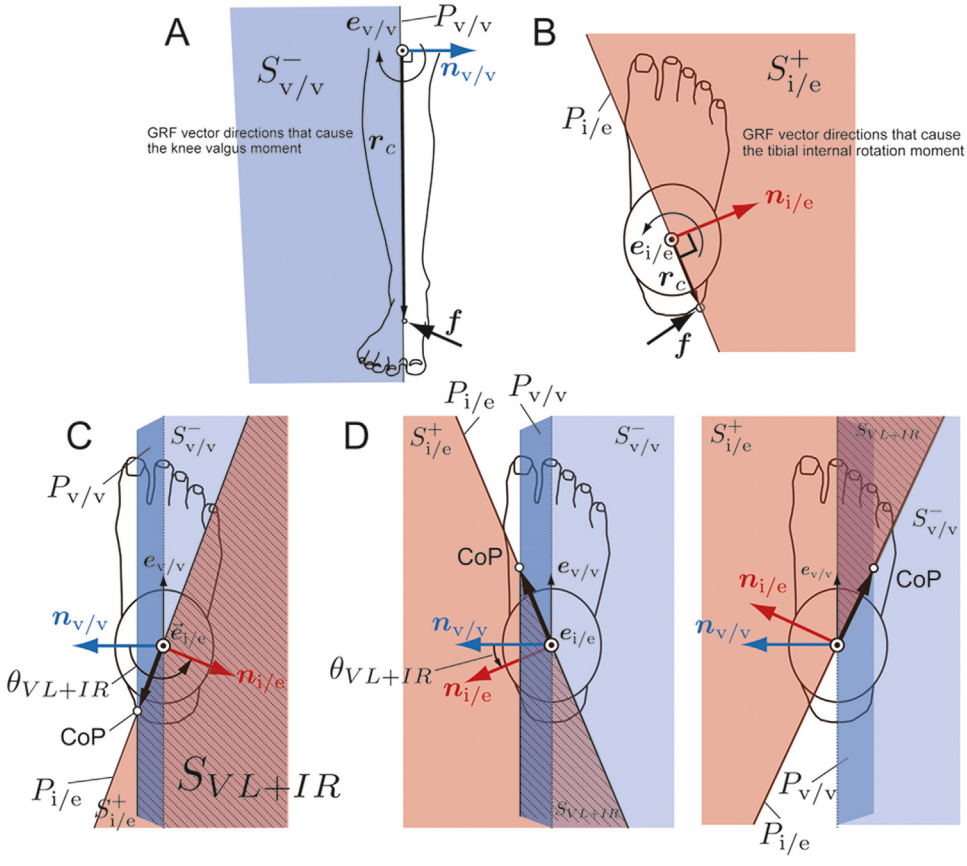

Fig. 2. (A) The space $S^{-}_{\mathrm{v/v}}$ (blue space) represents the GRF vector directions to cause the knee VL moment; (B) The space $S^{+}_{\mathrm{i/e}}$ (red space) represents the GRF directions to cause the tibial IR moment; (C) When the GRF vector points to the overlapped space S_{VL+IR} (stripe pattern space), the combined VL + IR moment applies at the knee. The volume of the space S_{VL+IR} is maximized when the CoP is posterior to the tibial rotational axis and the 2 unit normal vectors ($\boldsymbol{n}_{\mathrm{v/v}}$ and $\boldsymbol{n}_{\mathrm{i/e}}$) make large angle; (D) When the CoP is anterior to the tibial rotational axis, a small space S_{VL+IR} appears at anterior or posterior of the tibial rotational axis. CoP = center of pressure; GRF = ground reaction force; IR = internal rotation; VL = valgus.

Please cite this article as: Issei Ogasawara et al., The deterministic condition for the ground reaction force acting point on the combined knee valgus and tibial internal rotation moments in early phase of cutting maneuvers in female athletes, Journal of Sport and Health Science (2024), https://doi.org/10.1016/j.jshs.2023.11.005

specify the S^+ and S^- side of each plane. For example, the space $S^+_{i/e}$ indicates separation by the plane $P_{i/e}$ and the positive direction of $\boldsymbol{n}_{i/e}$. Eqs. (6) and (7) denote that those normal vectors $\boldsymbol{n}_{v/v}$ and $\boldsymbol{n}_{i/e}$ are functions of the CoP position relative to the shank segment. The generation of the combined knee VL + IR moment is determined by the GRF vector orientation relative to the normal vectors $\boldsymbol{n}_{v/v}$ and $\boldsymbol{n}_{i/e}$. Substituting (1) for Eqs. (2) and (3) yields:

$$\tau_{v/v} = \boldsymbol{e}^T_{v/v}(\boldsymbol{r}_c \times \boldsymbol{f}) \quad \text{Eq. (8)}$$

for knee varus/valgus moment and

$$\tau_{i/e} = \boldsymbol{e}^T_{i/e}(\boldsymbol{r}_c \times \boldsymbol{f}) \quad \text{Eq. (9)}$$

for tibial internal/external rotation moment. With the scalar triple product and Eqs. (6) and (7), Eqs. (8) and (9) can be rewritten as

$$\tau_{v/v} = \boldsymbol{f}^T(\boldsymbol{e}_{v/v} \times \boldsymbol{r}_c)$$

$$= \boldsymbol{f}^T \boldsymbol{n}_{v/v} \parallel \boldsymbol{e}_{v/v} \times \boldsymbol{r}_c \parallel \quad \text{Eq. (10)}$$

for knee varus/valgus moment and

$$\tau_{i/e} = \boldsymbol{f}^T\left(\boldsymbol{e}_{i/e} \times \boldsymbol{r}_c\right) = \boldsymbol{f}^T \boldsymbol{n}_{v/v} \parallel \boldsymbol{e}_{v/v} \times \boldsymbol{r}_c \parallel \quad \text{Eq. (11)}$$

for tibial internal/external rotation moment. Since $\|\boldsymbol{e}_{v/v} \times \boldsymbol{r}_c\|$ and $\|\boldsymbol{e}_{i/e} \times \boldsymbol{r}_c\|$ are non-negative, Eqs. (10) and (11) suggest that the orientation of the GRF vector relative to the unit normal vectors $\boldsymbol{f}^T\boldsymbol{n}_{v/v}$ and $\boldsymbol{f}^T\boldsymbol{n}_{i/e}$ determines the sign of the knee varus/valgus $\tau_{v/v}$ and tibial internal/external rotation moment $\tau_{i/e}$, respectively. The GRF vector which satisfies both

$$\boldsymbol{f}^T \boldsymbol{n}_{v/v} < 0 \quad \text{Eq. (12)}$$

and

$$\boldsymbol{f}^T \boldsymbol{n}_{i/e} > 0 \quad \text{Eq. (13)}$$

applies the VL + IR moment. Eqs. (12) and (13) intuitively visualize the 3D GRF vector directions that cause the combined knee VL + IR moment as a space delimited by 2 planes (Fig. 2). Eq. (12) means that GRF vectors point to the space $S^-_{v/v}$ (blue colored space in Fig. 2A) to apply the knee valgus moment. Eq. (13) similarly represents that GRF vectors point to the space $S^+_{i/e}$ (red colored space in Fig. 2B) to apply the tibial internal rotation moment. Finally, the space S_{VL+IR}, which is a spatial overlap between $S^-_{v/v}$ and $S^+_{i/e}$ (stripe pattern space in Fig. 2C and 2D), shows how the GRF vector directions apply the VL + IR moments simultaneously. The size of the overlapped space S_{VL+IR} is also a function of CoP position. When the CoP is posterior to the tibial rotational axis ($\boldsymbol{e}^T_{v/v}\boldsymbol{r}_c < 0$), and as the angle between $\boldsymbol{n}_{v/v}$ and $\boldsymbol{n}_{i/e}$ (i.e., $\theta_{VL+IR} = \cos^{-1}\left(\frac{\boldsymbol{n}^T_{v/v}\boldsymbol{n}_{i/e}}{\|\boldsymbol{n}_{v/v}\|\|\boldsymbol{n}_{i/e}\|}\right)$) becomes close to π rad, a large space S_{VL+IR} appears laterally to the shank segment (Fig. 2C). In contrast to the posterior case, if the CoP is anterior to the tibial rotational axis ($\boldsymbol{e}^T_{v/v}\boldsymbol{r}_c > 0$) as the angle θ_{VL+IR} becomes close to 0 rad, a small S_{VL+IR} appears anteriorly or posteriorly to the shank segment (Fig. 2D). This deterministic mechanical condition suggests a high likelihood of occurrence of the combined knee VL + IR moment if the GRF vector stochastically points to the enlarged space S_{VL+IR} while the CoP is posterior to the tibial rotational axis in sports movement.

2.2. Experimental verification of the stochastic aspect of the combined knee VL + IR moment occurrence

2.2.1. Participants

Fourteen healthy collegiate female handball players (height = 161.5 ± 3.4 cm; weight = 55.4 ± 5.6 kg; and age = 21.0 ± 0.8 years (mean ± SD)) participated in this study. Athletes who had a history of lower limb musculoskeletal injuries within the 6 months leading up to the experiment or knee injuries requiring surgery, such as ACL rupture, were excluded. The local ethics board approved this experiment (Mukogawa Women's University, No. 12−13), and written informed consent was obtained from all participants. This research was performed in accordance with all relevant guidelines and in accordance with the Declaration of Helsinki.

2.2.2. Motor task and data collection

The experimental protocol was previously reported elsewhere.[28] Briefly, participants underwent the 60° change-of-direction (cutting) task with their ipsilateral leg on the force plate. The leg used for cutting was defined as the preferred leg to control the foot posture at foot-floor impact, and all participants selected their right leg for the experiment. The reference cone was placed on the floor at an angle of 60° from the approach line to show the cutting destination.

Cuttings were executed under the 2 following foot-strike conditions to differentiate the position of CoP. For the rearfoot strike condition, participants hit the force plate with their heel first, to place the CoP posterior to the tibial rotational axis at foot impact, and then shifted their weight toward the forefoot for propulsion. In the forefoot strike condition, the participants were asked to touch the force plate with their forefoot (around the ball of foot) throughout the stance phase. The relatively slow approach speed of <2.0 m/s was used in this experiment. The reason for the slow approach speed was to reduce the magnitude of GRF to ensure participants' safety, especially in the rearfoot strike condition.[28]

Sixteen reflective markers (diameter = 14 mm) were attached to 16 bony landmarks (Table 1) using double-sided adhesive tape. Participants familiarized themselves to the task requirements: the cutting angle of 60°, the approach speed of <2.0 m/s, and the correct foot placements on the force plate for the 2 foot-strike conditions. The speed of the mid-point of both anterior superior iliac spine markers was calculated in real-time using the data streaming function of the motion capture software (NatNet in Motive Body 1.1; NaturalPoint, Inc., Corvallis, OR, USA) combined with custom LabVIEW script (National Instruments Corp., Austin, TX, USA), and feedback was given to participants to adjust the approach

Please cite this article as: Issei Ogasawara et al., The deterministic condition for the ground reaction force acting point on the combined knee valgus and tibial internal rotation moments in early phase of cutting maneuvers in female athletes, Journal of Sport and Health Science (2024), https://doi.org/10.1016/j.jshs.2023.11.005

Table 1
Locations of body markers on the cutting limb and pelvis.

Toe	On the most anterior point of the shoe toe
Medial toe	Medial aspect of the most prominent point of the first MP joint over the sports shoe
Lateral toe	Lateral aspect of the most prominent point of the fifth MP joint over the sports shoe
Forefoot	Dorsal aspect of the midpoint of the second and third MP joint over the sports shoe
Medial ankle	On the most prominent point of the medial malleolus
Lateral ankle	On the most prominent point of the lateral malleolus
Heel	On the most posterior point of the shoe heel and 2 cm above the floor level when the subject is standing stationary
Medial knee	On the most prominent point of the medial femoral epicondyle
Lateral knee	On the most prominent point of the lateral femoral epicondyle
Anterior knee	On the most prominent point of the tibial tuberosity
Mid shank	On the approximately halfway of the anterior aspect of the shank; the marker was located on the skinny region on the tibia to avoid skin fluctuation
Great trochanter	On the most prominent point of the great trochanters (both sides)
Mid thigh	On the approximately halfway of the anterior aspect of the thigh
ASIS	On the most prominent point of the anterior superior iliac spines (both sides)

Abbreviations: ASIS = anterior superior iliac spine; MP = metatarsophalangeal.

speed to <2.0 m/s. After task familiarization, a total of 10 trials for each foot-strike condition were measured. The order of the 2 foot-strike conditions was randomized for each participant to equalize the effects of fatigue between the foot-strike conditions. A 3-min rest between conditions and approximately 30-s intervals between trials also minimized the effects of fatigue. The 3D positions of reflective markers were collected using 12 optical cameras (OptiTrack S250e, with 250-Hz sampling; NaturalPoint, Inc.) and software (Motive Body 1.1; NaturalPoint, Inc.). GRF data were collected with Kistler Type 9281B (1 kHz sampling; Kistler, Winterthur, Switzerland) and synchronized with OptiTrack using the clock device (eSync2; NaturalPoint, Inc.). Any trial that exceeded the approach speed of 2.0 m/s would be regarded as an error trial; however, no trials exceeded 2.0 m/s during the data collection process.

2.2.3. Data processing

The position data were smoothed with a second-order Butterworth digital filter (low-pass, zero-lag, and cutoff-frequency 12−15 Hz). The GRF data were smoothed with a second-order Butterworth digital filter with cutoff-frequencies of 70 Hz[29] and then resampled at 250 Hz with spline interpolation. The calculation of the model is detailed in the Supplemental Table 1. The knee varus/valgus and tibial internal/external rotational moments due to GRF were calculated using Eqs. (2) and (3). These moments were represented with respect to the SCS Σ^S. To investigate the directional distribution of the horizontal GRF vector component relative to the shank segment, the horizontal GRF vector in the GCS Σ^O was transformed to the SCS Σ^S as follows:

$$\boldsymbol{f}_h^S = \begin{bmatrix} f_x^S \\ f_y^S \\ 0 \end{bmatrix} = \boldsymbol{E}_h \boldsymbol{R}^S \boldsymbol{f}, \quad \text{Eq. (14)}$$

where the subscript h denotes horizontal and

$$E_h = \begin{bmatrix} 1 & 0 & 0 \\ 0 & 1 & 0 \\ 0 & 0 & 0 \end{bmatrix} \quad \text{Eq. (15)}$$

is a matrix to extract the horizontal component of GRF vector with respect to the SCS Σ^S.

2.2.4. Statistical analysis

The speed of the mid-point of both anterior superior iliac spine markers averaged from −40 to 0 ms prior to foot impact. Speeds were compared between foot-strike conditions using paired t tests ($p < 0.05$) to ensure that approach speeds did not differ between foot-strike conditions. The time points of interest were defined every 10 ms, from 0 to 100 ms after foot impact. This period (0−100 ms) was selected based on prior evidence that reported an increased occurrence of ACL injuries within the aforementioned time window.[8] At each time point, all trials ($n = 280$) were divided into 2 trial groups, depending on the instantaneous CoP position as,

$$\textit{trial group} = \begin{cases} \textit{anterior CoP}, & \boldsymbol{e}_{\mathrm{v/v}}^T \boldsymbol{r}_c > 0 \\ \textit{posterior CoP}, & \boldsymbol{e}_{\mathrm{v/v}}^T \boldsymbol{r}_c < 0. \end{cases} \quad \text{Eq. (16)}$$

Occurrence rates of the combined knee VL + IR moment were calculated by dividing the count of trials satisfying both $\boldsymbol{f}^T \boldsymbol{n}_{\mathrm{v/v}} < 0$ and $\boldsymbol{f}^T \boldsymbol{n}_{\mathrm{i/e}} > 0$ by the number of total trials in each trial group. χ^2-squared tests ($p < 0.05$) were performed to examine whether the occurrence rate was significantly different between groups (anterior CoP *vs*. posterior CoP) at each time point.

To compare the directional distribution of the horizontal GRF vector components with respect to the SCS between trial groups, the angle $\psi_{GRF,h}$ (angle between the horizontal GRF vector $\boldsymbol{f}_h^S$ and unit vector $\boldsymbol{e}_{\mathrm{v/v}}$, $0 \leq \psi_{GRF,h} < 2\pi$ rad) was calculated and compared with the Watson's U^2 test ($p < 0.05$) for both trial groups at each time point.[30] The time course change of the directional distribution of the horizontal GRF vector was not the focus of this study, and since we considered each time point to be independent, the correction of p value was not performed in the Watson's U^2 test.

3. Results

3.1. Approach speed

The approach speeds did not differ significantly between the 2 foot-strike conditions (1.47 ± 0.13 m/s *vs*. 1.46 ± 0.11 m/s for forefoot and rearfoot strike conditions, respectively; $p = 0.71$).

Please cite this article as: Issei Ogasawara et al., The deterministic condition for the ground reaction force acting point on the combined knee valgus and tibial internal rotation moments in early phase of cutting maneuvers in female athletes, Journal of Sport and Health Science (2024), https://doi.org/10.1016/j.jshs.2023.11.005

3.2. Descriptive explanation of the deterministic results from the representative trials

The representative trials for each foot-strike condition are shown in Fig. 3. For the rearfoot strike condition, the combined knee VL + IR moment occurred from 0 to 0.09 s (Fig. 3A) while the CoP was posterior to the tibial rotational axis ($\boldsymbol{e}_{v/v}^{T}\boldsymbol{r}_c < 0$, Fig. 3C). In the forefoot strike condition, the CoP was always anterior to the tibial rotational axis (Fig. 3D), and the combined knee VL + IR moment did not occur throughout the stance (Fig. 3B). The angles θ_{VL+IR} between $\boldsymbol{n}_{v/v}$ and $\boldsymbol{n}_{i/e}$ in both foot-strike conditions were shown to represent the volume of the space S_{VL+IR} (Fig. 3E and 3F). Again, as the angle θ_{VL+IR} approached π rad, the volume of the space S_{VL+IR} is maximized as theorized above. The angle θ_{VL+IR} was larger than $\pi/2$ rad only when the CoP was posterior to the tibial rotational axis in the early stance phase of the rearfoot strike condition (Fig. 3C and E) and the large space S_{VL+IR} appeared at the posterolateral region of the shank segment (Fig. 3G). The GRF vector pointed to the enlarged space

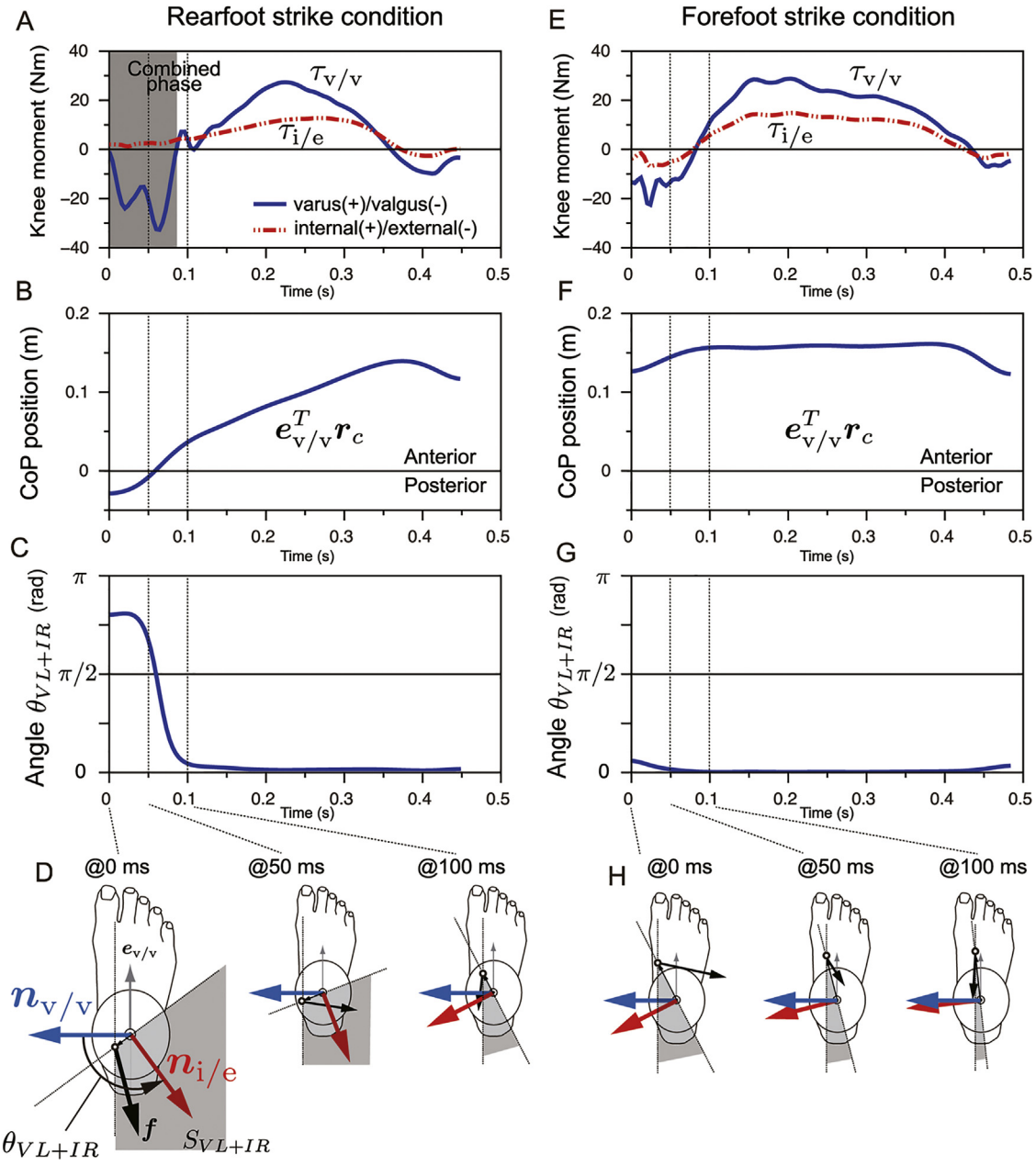

Fig. 3. The representative data from both foot strike conditions. (A and B) The combined knee VL and IR moment occurred when the CoP was posterior to the tibial rotational axis in the rearfoot contact condition; (C and D) The posterior-CoP created a large angle θ_{VL+IR} between the normals $\boldsymbol{n}_{v/v}$ and $\boldsymbol{n}_{i/e}$, indicating that the large space S_{VL+IR} appeared postero-lateral to the shank segment. The GRF vector went inside the space S_{VL+IR} at 0 and 50 ms and applied the combined knee VL + IR moment, whereas it was outside of the space S_{VL+IR} at 100 ms; thus, the knee VL + IR combination disappeared; (E and F) In the forefoot strike condition, the knee VL and tibial IR moments did not combine throughout the stance and the CoP was always anterior to the tibial rotational axis; (G and H) The small angle θ_{VL+IR} between the normals $\boldsymbol{n}_{v/v}$ and $\boldsymbol{n}_{i/e}$ created a small space S_{VL+IR}, and the GRF vector consistently directed outside of the space S_{VL+IR}. CoP = center of pressure; GRF = ground reaction force; IR = internal rotation; VL = valgus.

Please cite this article as: Issei Ogasawara et al., The deterministic condition for the ground reaction force acting point on the combined knee valgus and tibial internal rotation moments in early phase of cutting maneuvers in female athletes, Journal of Sport and Health Science (2024), https://doi.org/10.1016/j.jshs.2023.11.005

S_{VL+IR} at 0 and 50 ms, whereas it directed outside at 100 ms (Fig. 3G), which temporally corresponded with the occurrence of the combined knee VL + IR moment (Fig. 3A). In contrast, in the forefoot strike condition, the angle θ_{VL+IR} was nearly 0 rad throughout the stance phase, and thus the volume of the space S_{VL+IR} was small (Fig. 3F and 3H). The GRF vector did not point to the space S_{VL+IR}; therefore, the combined knee VL + IR moment did not occur.

3.3. Occurrence rate of the combined knee VL + IR moment between different CoP positions

Our participants successfully reproduced posterior-CoPs in >80% of the total trials in the rearfoot strike condition from 0 to 40 ms after foot strike (Fig. 4). The number of posterior-CoP trials in the rearfoot strike condition gradually decreased as the CoP moved from rearfoot to forefoot across the tibial rotational axis. The forefoot strike condition did not show any posterior-CoP trials throughout the time points of interest. χ^2 tests showed that the occurrence rate of combined knee VL + IR moments in the posterior-CoP trial group was significantly higher than that of the anterior-CoP trial group at every time point of interest ($p < 0.05$, Fig. 5). The posterior-CoP trial group had particularly high occurrence rates of 82.8% and 61.5% at 0 and 10 ms after foot strikes, respectively, whereas the anterior-CoP trial group showed low occurrence rates of 2.1% and 22.1% at the same time points.

3.4. Directional distribution of the horizontal GRF vector component among trial groups

The horizontal GRF vector generally directed laterally to the shank segment for both anterior- and posterior-CoP trial groups from 0 to 100 ms (Fig. 6A). At 10−40 ms, the posterior-CoP trials in the rearfoot-strike condition showed the anteriorly directed GRF vector components, while the anterior-CoP trials exhibited posteriorly directed components. The Watson's U^2 test demonstrated that there was a significant directional difference in the horizontal GRF vectors between anterior- and posterior-CoP trial groups at 20 ms after foot strike (Fig. 6B *vs.* Fig. 6C). Most of the horizontal GRF components from the posterior-CoP trials pointed to the possible range of the space S_{VL+IR}, especially from 0 to 40 ms, while the horizontal GRF vector in the anterior-CoP trials directed outside of the possible range of the space S_{VL+IR} at the same time points.

4. Discussion

This study is the first to identify the deterministic mechanical condition explaining the relationship between CoP position (GRF vector acting point within the base of support of the stance foot) and the potential GRF vector directions, visualized as a space S_{VL+IR}, resulting in the combined knee VL + IR moment. Further, we empirically investigated the stochastic aspect of sport maneuver (cutting) relevant to this mechanical condition. The results indicated that cuttings tended to produce a laterally directed GRF vector relative to the shank segment, and when the rearfoot strikes located the CoP posteriorly to the tibial rotational axis, GRF vectors predominantly pointed to the enlarged space S_{VL+IR}. Consequently, cuttings with rearfoot strike increased the occurrence rate of the combined knee VL + IR moment. These findings reinforced our hypothesis.

Several studies discussing the mechanism of non-contact ACL injury have addressed how multi-directional combined loading is harmful for the ACL based on the ACL's anatomical biomechanics,[14,15] and some include video observations of injurious events.[8,31] However, the theoretical basis for the

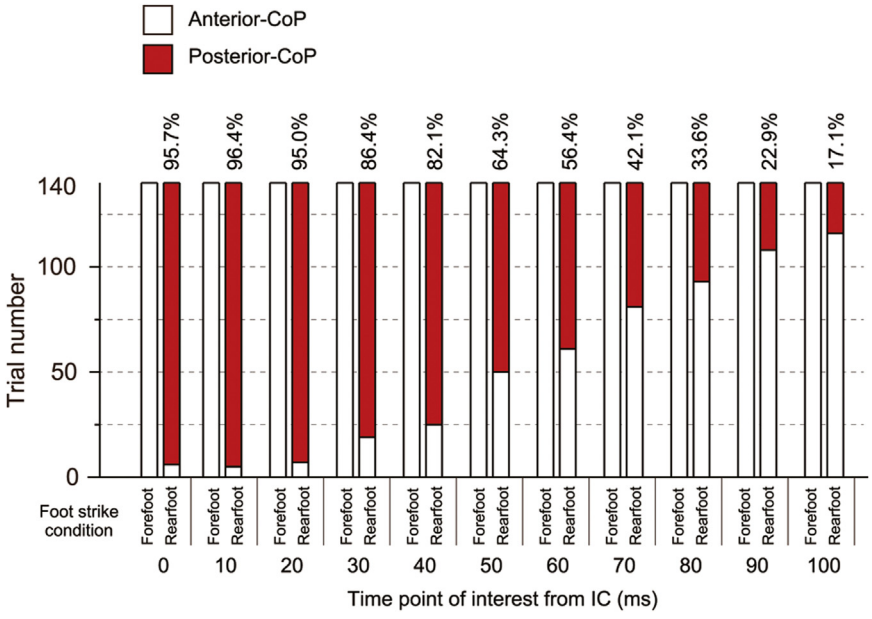

Fig. 4. The number of anterior- and posterior-CoP trials for both foot strike conditions is shown. More than 80% of total trials were posterior-CoP trials from 0 to 40 ms after IC. The number of the posterior-CoP trials gradually decreased as the CoP moved to the forefoot region. The forefoot strike condition did not create any posterior-CoP trials at every time point of interest. CoP = center of pressure; IC = initial foot contact.

Please cite this article as: Issei Ogasawara et al., The deterministic condition for the ground reaction force acting point on the combined knee valgus and tibial internal rotation moments in early phase of cutting maneuvers in female athletes, Journal of Sport and Health Science (2024), https://doi.org/10.1016/j.jshs.2023.11.005

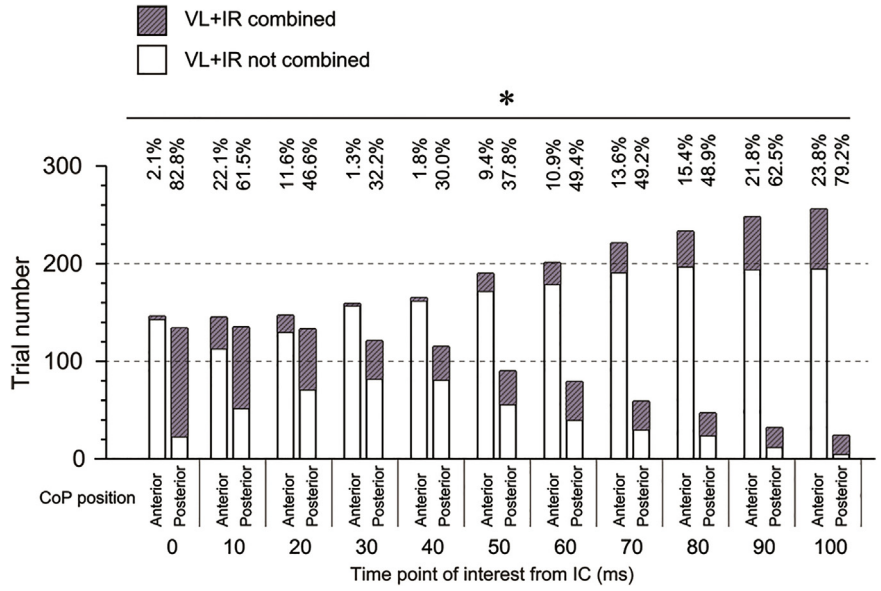

Fig. 5. The χ^2 test revealed that there were significant differences in the occurrence rates between the anterior- and posterior-CoP trials at every time point of interest (* $p < 0.05$). The posterior-CoP trials showed quite high rates of 82.8% and 61.5% at 0 and 10 ms after impact, whereas the anterior-CoP trials decreased the occurrence rates of <30% throughout the time points of interests. CoP = center of pressure; IC = initial foot contact; IR = internal rotation; VL = valgus.

development of the combined knee VL + IR moment and its association with sports-specific movements has been unclear. The key message of this study was that the foot-strike techniques inducing the posterior CoP, such as rearfoot strike, may be dangerous, especially during horizontal deceleration since it potentially adds the risk of non-contact ACL injury due to the combined knee VL + IR mechanism.

In this study, we specifically tested our hypothesis with the cutting motion since cutting (rapid deceleration and change-of-direction with the ipsilateral leg) is one of the inciting maneuvers for non-contact ACL injuries.[8,18,32] The posterior CoP created by rearfoot strike is expected to be particularly problematic when accompanying a maneuver that stochastically produces the laterally directed GRF vector relative to the shank segment. The occurrence of knee valgus moment due to the laterally directed GRF vector relative to the shank segment has been observed commonly in the early stance phase of cuttings.[20,21,28,33–36] Our participants consistently exhibited the laterally directed GRF vector regardless of foot-strike pattern (Fig. 6B and 6C), indicating that the demand of the cutting maneuver—a horizontal deceleration using a laterally planted leg—tends to induce the laterally directed GRF component with respect to the shank segment in females. The spatial congruity between the cutting-specific lateral GRF component and the enlarged space S_{VL+IR} that spans the lateral aspect of the shank segment due to posterior CoP (Figs. 2 and 6) is the mechanical reason for the increased likelihood of combined knee VL + IR moment occurrence during rearfoot-strike cuttings. This spatial congruity may be associated with the non-contact ACL injury mechanism occurring in rearfoot strike.[25,26,37] The movement-specific GRF vector direction in another relevant movement may be different from that of cuttings. For example, in ACL injury in single-legged landing,[17,18] the vertical GRF component may be a dominant contributor to injury development.[22,31,38] Regardless of the movement, a posterior CoP still expands a large space S_{VL+IR} at the lateral aspect of the shank segment; however, the probability that the GRF vector points to that space S_{VL+IR} in a single-legged landing is expected to be lower than in cutting. In addition, even if the GRF vector points to the space S_{VL+IR} in a single-legged landing, the horizontal GRF component that increases the magnitude of the knee valgus and tibial rotation moments becomes small. Therefore, in a more vertical deceleration movement, there are likely to be different primary injurious mechanisms, such as a high compressive force due to increased vertical GRF combined with posterior tibial slope.[38–40] The effect of CoP position on the multi-directional knee stress in a single-legged landing and its influence on the movement-specific ACL injury mechanism should be examined in a future study.

The different foot-strike conditions produced characteristic discrepancies in the stochastic GRF vector directional distributions from 10 ms to 30 ms (Fig. 6A). The GRF vector direction of the anterior-CoP trial group showed a posterior-lateral direction pointing outside of the space S_{VL+IR}. In contrast, the posterior-CoP trial group showed one with an anterior-lateral direction pointing to the space S_{VL+IR} (Fig. 6B and 6C). Given that all anterior-CoP trials were from forefoot strikes whereas >80% of posterior-CoP trials were produced by rearfoot strikes (Fig. 4), the directional discrepancy along anterior-posterior lines in the GRF vector relative to the tibial rotational axis was attributed to the foot-strike pattern difference.[23] Although the Watson's U^2 test identified the statistically significant difference in GRF vector directional distributions between anterior- and posterior-CoP trial groups only at the 20 ms time point (Fig. 6A), considering the function of the ACL, the opposite GRF vector in the anterior−posterior direction may produce an opposite effect on ACL stress around this

Please cite this article as: Issei Ogasawara et al., The deterministic condition for the ground reaction force acting point on the combined knee valgus and tibial internal rotation moments in early phase of cutting maneuvers in female athletes, Journal of Sport and Health Science (2024), https://doi.org/10.1016/j.jshs.2023.11.005

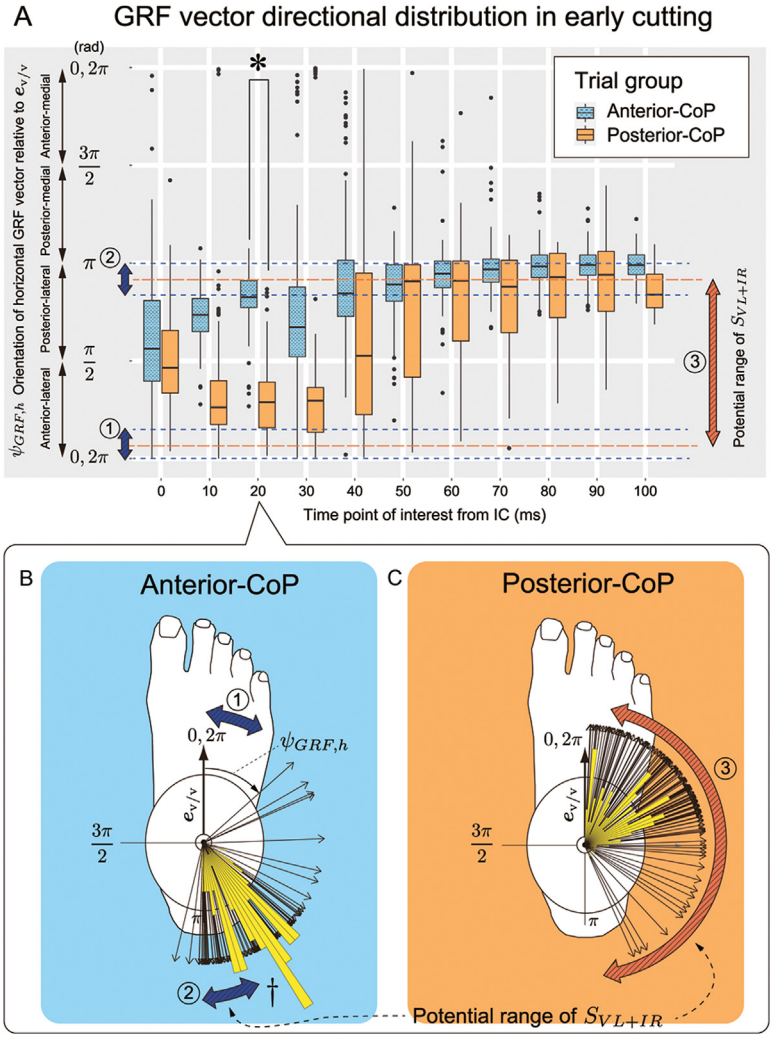

Fig. 6. The directional distribution of the horizontal GRF vector components with respect to the shank coordinate system. The direction of horizontal GRF vector relative to the varus/valgus axis $\boldsymbol{e}_{v/v}$ was expressed as angle $\psi_{GRF,\,h}$. The value of angle increases clockwise. (A) Illustration of the time-course change of horizontal GRF vector components of the anterior- and posterior-CoP groups. Additionally, the possible ranges of space S_{VL+IR} were provided separately when the CoP is anterior (blue-stripe color arrows ① and ②, $\boldsymbol{e}_{v/v}^{T}\boldsymbol{r}_c > 0$) and posterior (orange arrow ③, $\boldsymbol{e}_{v/v}^{T}\boldsymbol{r}_c < 0$) to the tibial rotational axis. Important finding from this result was that the most of horizontal GRF vector in the posterior-CoP trials occurred during rearfoot strike condition pointed to the possible range of S_{VL+IR} from 0 to 40 ms after foot strike, whereas the anterior-CoP trials from the forefoot strike condition did not; (B and C) The circular histograms visually compared the directional distribution difference between anterior- and posterior-CoP trials with the possible range of S_{VL+IR} at 20 ms (Watson's U^2 test, * $p < 0.05$). † denotes that in anterior-CoP trial group, the GRF vectors caused the combined knee VL + IR moment directed posterior-lateral of the shank segment. In contract, for the posterior-CoP trial group, the GRF vectors caused the combined knee valgus and tibial internal rotation moment directed anterior-lateral of the shank segment. CoP = center of pressure; GRF = ground reaction force; IC = initial foot contact; IR = internal rotation; VL = valgus.

same time point. The non-contact ACL injuries have been reported as occurring approximately 30−40 ms after initial foot contact (IC),[31,41] and this time frame for ACL injury is slightly after the period during which our data illustrated the directional discrepancies in the horizontal GRF vectors between fore and rearfoot strikes (Fig. 6A). Based on 10 actual ACL injuries (including 7 cutting cases) in females, Koga et al.[31] conceptualized a detailed mechanism of ACL injury involving knee valgus and subsequent tibial internal rotation. Further, Koga et al.[41] reported 1 male ACL injury that showed a drastic increase of tibial anterior translation (relative femoral posterior dislocation) at the first 30 ms after rearfoot strike. To rupture the ACL within 40 ms under such 3D stress, the knee VL moment, tibial IR moment, and tibial anterior translation forces must act before 40 ms from IC. When we focus only on the GRF vectors measured in this study, the GRF vectors seen in the posterior-CoP trial group at 10−30 ms after rearfoot strike, which directed anterolateral and pointed to the space S_{VL+IR}, would be the source of these forces since the anterior GRF component relative to the tibial axis has been known to generate the tibial anterior translation force[22] and more frequently occurs at rearfoot strike in cuttings.[23] Therefore, the different GRF directions and CoP locations associated with the foot-strike pattern difference can be explained in terms of the precursor mechanics that foster the eventual 3D mechanism of non-contact ACL injury.

The combined knee VL + IR moment also occurred in the forefoot strikes (anterior CoP); however, it is speculated that

stress on the ACL is opposite here than in the rearfoot strikes (posterior CoP) due to the differences in the anterior-posterior component of the GRF vector relative to the tibial rotational axis. Even the anterior-CoP trial group produced by forefoot strikes exhibited 9.4%−23.8% of the combined knee VL + IR moment occurrence rate from 50 ms to 100 ms after foot impact (Fig. 5). This result was caused by the posterior-laterally directed GRF vectors captured by the small space S_{VL+IR}, which appeared at the posterior aspect of the shank (See dagger in Fig. 6). These results show that even if the CoP is anterior to the tibial rotational axis, the probability of the combined knee VL + IR occurrence cannot be reduced to 0 as long as the space S_{VL+IR} exists (Fig. 2). However, if the posteriorly directed GRF vector produced the combined knee VL + IR moment, it may also produce a posterior shear force at the knee[42,43] and may reduce the mechanical stress on the ACL.

Note that the deterministic mechanical condition visualized in Fig. 2 does not adhere to the type of sports maneuvers and sex of athletes, as the equation of motion can be applied to any types of sport maneuvers and both sexes. The abstractness of this concept helps generalize our conclusion to the mechanics of any sport movements associated with combined knee VL + IR stress-driven ACL injury and its prevention. For example, this concept may explain the reason the video observational evidence reports the opposite: a high ACL injury rate in heel strikes[24,25] while forefoot landing was consistent in similar situations but did not result in ACL injury.[26,27] In the context of prevention, once a sports practitioner acquires the concept, they may be able to design a suitable foot strike technique and associated whole-body configuration during cutting or landing that can limit the GRF vector's directional probability for causing the combined knee VL + IR moment. A concrete example of technical training is acquiring forefoot-first landings. The forefoot-first landing diminishes the opportunity to locate the CoP at the rearfoot. Consequently, it reduces the probability of combined knee VL + IR stress because the size of space S_{VL+IR} will be minimized as long as the CoP is at the forefoot. The correct foot placement relative to the body center of mass is also a vital biomechanical factor for a stable forefoot landing. A foot placement that is so far forward from the body center of mass that the tibia is tilted backward will induce a rearfoot strike. Therefore, it is essential to master positioning the foot appropriately closer to the body center of mass.

This study has limitations. Our theory only considered the moment of GRF and omitted the other external moment terms from Euler's equation of motion (i.e., rotational inertia moment, friction moment, and gravity moment). However, previous studies suggested that the moment of GRF is the primary determinant of the dynamics of the femur−tibia link system because, during cutting, the magnitude of GRF becomes significant relative to other external forces.[44,45] Our experiment used a single-sex design to exclude the known sex differences in knee kinetics during cuttings; therefore, the occurrence rate of the combined knee VL + IR moment may be lower in male athletes since the literature demonstrated that male athletes did not exhibit the knee valgus moment in the early deceleration phase during cutting.[46] It is logically expected that such a GRF vector would point out of the space S_{VL+IR} even when the CoP is posterior to the tibial rotational axis. Future studies should do a sex comparison of the effect of CoP position on the combined knee VL + IR moment.

5. Conclusion

Our study theoretically identified how different CoP positions affect the range of GRF vector directions for applying the combined knee VL + IR moment wherein posterior-CoP increases the GRF vector's directional probability for causing said moment. We empirically found that in the early phase of cutting maneuvers in female athletes, rearfoot strikes tended to create a posterior CoP relative to the tibial rotational axis and so produced the combined knee VL + IR moment more frequently than did the anterior-CoP. Although an epidemiological verification will be needed, adapting the forefoot strike technique as opposed to the rearfoot strike technique may become a practical strategy for reducing the risk of non-contact ACL injury due to the combined knee VL + IR moment mechanism.

Acknowledgments

This work was supported by the Grant-in-Aid for Young Scientists (B) Project (Grant No. 24700716) funded by the Ministry of Education, Culture, Sports, Science and Technology, Japan.

Authors' contributions

IO conceived, planned, and designed the study, acquired and interpreted the data, and drafted and edited the manuscript; KO conceived, planned, and designed the study, and supervised the mathematical modelling; GSR drafted and edited the manuscript; SK drafted and edited the manuscript; YS planned and designed the study, supervised from ACL injury research perspective, and critically appraised the manuscript; HK supervised from an ACL injury research perspective and critically appraised the manuscript; KN supervised from an ACL injury research perspective. All authors have read and approved the final manuscript, and agree with the order of presentation of the authors.

Competing interests

The authors declare that they have no competing interests.

Availability of data and materials

Data that support the findings of this study will be made available from the corresponding author upon reasonable request.

References

1. Butler DL, Noyes FR, Grood ES. Ligamentous restraints to anterior-posterior drawer in the human knee. A biomechanical study. *J Bone Joint Surg Am* 1980;**62**:259–70.
2. Pandy MG, Shelburne KB. Dependence of cruciate-ligament loading on muscle forces and external load. *J Biomech* 1997;**30**:1015–24.
3. Isaac DL, Beard DJ, Price AJ, Rees J, Murray DW, Dodd CAF. *In-vivo* sagittal plane knee kinematics: ACL intact, deficient and reconstructed knees. *Knee* 2005;**12**:25–31.

4. Bere T, Flørenes TW, Krosshaug T, et al. Mechanisms of anterior cruciate ligament injury in World Cup alpine skiing: A systematic video analysis of 20 cases. *Am J Sports Medicine* 2011;**39**:1421–9.
5. Schilaty ND, Bates NA, Krych AJ, Hewett TE. Frontal plane loading characteristics of medial collateral ligament strain concurrent with anterior cruciate ligament failure. *Am J Sports Med* 2019;**47**:2143–50.
6. Bates NA, Nesbitt RJ, Shearn JT, Myer GD, Hewett TE. Knee abduction affects greater magnitude of change in ACL and MCL strains than matched internal tibial rotation i*n vitro*. *Clin Orthop Relat Res* 2017;**475**:2385–96.
7. Kanamori A, Zeminski J, Rudy TW, Li G, Fu FH, Woo SL-Y. The effect of axial tibial torque on the function of the anterior cruciate ligament: A biomechanical study of a simulated pivot shift test. *Arthrosc J Arthrosc Relat Surg* 2002;**18**:394–8.
8. Krosshaug T, Nakamae A, Boden BP, et al. Mechanisms of anterior cruciate ligament injury in basketball: Video analysis of 39 cases. *Am J Sports Med* 2007;**35**:359–67.
9. Villa FD, Buckthorpe M, Grassi A, et al. Systematic video analysis of ACL injuries in professional male football (soccer): Injury mechanisms, situational patterns and biomechanics study on 134 consecutive cases. *Br J Sports Med* 2020;**54**:1423–32.
10. Ireland ML. Anterior cruciate ligament injury in female athletes: Epidemiology. *J Athl Train* 1999;**34**:150–4.
11. Quatman CE, Quatman-Yates CC, Hewett TE. A "Plane" explanation of anterior cruciate ligament injury mechanisms. *Sports Med* 2010;**40**:729–46.
12. Shimokochi Y, Shultz SJ. Mechanisms of noncontact anterior cruciate ligament injury. *J Athl Train* 2008;**43**:396–408.
13. Kanamori A, Woo S, Ma C, et al. The forces in the anterior cruciate ligament and knee kinematics during a simulated pivot shift test: A human cadaveric study using robotic technology. *Arthroscopy* 2000;**16**:633–9.
14. Markolf KL, Burchfield DM, Shapiro MM, Shepard MF, Finerman GA, Slauterbeck JL. Combined knee loading states that generate high anterior cruciate ligament forces. *J Orthop Res* 1995;**13**:930–5.
15. Oh YK, Lipps DB, Ashton-Miller JA, Wojtys EM. What strains the anterior cruciate ligament during a pivot landing? *Am J Sports Med* 2012;**40**:574–83.
16. Levine JW, Kiapour AM, Quatman CE, et al. Clinically relevant injury patterns after an anterior cruciate ligament injury provide insight into injury mechanisms. *Am J Sports Med* 2013;**41**:385–95.
17. Boden BP, Dean GS, Feagin JAJ, Garrett WEJ. Mechanisms of anterior cruciate ligament injury. *Orthopedics* 2000;**23**:573–8.
18. Olsen O-E, Myklebust G, Engebretsen L, Bahr R. Injury mechanisms for anterior cruciate ligament injuries in team handball: A systematic video analysis. *Am J Sports Med* 2004;**32**:1002–12.
19. Dempsey AR, Elliott BC, Munro BJ, Steele JR, Lloyd DG. Whole body kinematics and knee moments that occur during an overhead catch and landing task in sport. *Clin Biomech (Bristol, Avon)* 2012;**27**:466–74.
20. Sigward SM, Powers CM. Loading characteristics of females exhibiting excessive valgus moments during cutting. *Clin Biomech (Bristol, Avon)* 2007;**22**:827–33.
21. McLean SG, Huang X, van den Bogert AJ. Association between lower extremity posture at contact and peak knee valgus moment during sidestepping: Implications for ACL injury. *Clin Biomech (Bristol, Avon)* 2005;**20**:863–70.
22. Shimokochi Y, Ambegaonkar JP, Meyer EG. Changing sagittal-plane landing styles to modulate impact and tibiofemoral force magnitude and directions relative to the tibia. *J Athl Train* 2016;**51**:669–81.
23. Uno Y, Ogasawara I, Konda S, et al. Effect of the foot-strike pattern on the sagittal plane knee kinetics and kinematics during the early phase of cutting movements. *J Biomech* 2022;**136**:111056. doi:10.1016/j.jbiomech.2022.111056.
24. Koga H, Nakamae A, Shima Y, Bahr R, Krosshaug T. Hip and ankle kinematics in noncontact anterior cruciate ligament injury situations: Video analysis using model-based image matching. *Am J Sports Med* 2018;**46**:333–40.
25. Montgomery C, Blackburn J, Withers D, Tierney G, Moran C, Simms C. Mechanisms of ACL injury in professional rugby union: A systematic video analysis of 36 cases. *Br J Sports Med* 2016;**52**:994–1001.
26. Boden BP, Torg JS, Knowles SB, Hewett TE. Video analysis of anterior cruciate ligament injury. *Am J Sports Med* 2009;**37**:252–9.
27. Sheehan FT, Sipprell 3rd WH, Boden BP. Dynamic sagittal plane trunk control during anterior cruciate ligament injury. *Am J Sports Med* 2012;**40**:1068–74.
28. Ogasawara I, Shimokochi Y, Mae T, Nakata K. Rearfoot strikes more frequently apply combined knee valgus and tibial internal rotation moments than forefoot strikes in females during the early phase of cutting maneuvers. *Gait Posture* 2020;**76**:364–71.
29. Ogasawara I, Nambo M, Uno Y, et al. The counteracting effect of the friction moment against the tibial rotational moment driven by the ground reaction force in an early stance phase of cutting maneuver among healthy male athletes. *J Sport Sci* 2022;**40**:2072–84.
30. Landler L, Ruxton GD, Malkemper EP. Advice on comparing two independent samples of circular data in biology. *Sci Rep* 2021;**11**:20337. doi:10.1038/s41598-021-99299-5.
31. Koga H, Nakamae A, Shima Y, et al. Mechanisms for noncontact anterior cruciate ligament injuries. *Am J Sports Med* 2010;**38**:2218–25.
32. Hewett TE, Torg JS, Boden BP. Video analysis of trunk and knee motion during non-contact anterior cruciate ligament injury in female athletes: Lateral trunk and knee abduction motion are combined components of the injury mechanism. *Br J Sport Med* 2009;**43**:417–22.
33. Besier TF, Lloyd DG, Ackland TR, Cochrane JL. Anticipatory effects on knee joint loading during running and cutting maneuvers. *Med Sci Sports Exerc* 2001;**33**:1176–81.
34. Cortes N, Morrison S, Van Lunen BL, Onate JA. Landing technique affects knee loading and position during athletic tasks. *J Sci Med Sport* 2012;**15**:175–81.
35. Dempsey AR, Lloyd DG, Elliott BC, Steele JR, Munro BJ. Changing sidestep cutting technique reduces knee valgus loading. *Am J Sports Med* 2009;**37**:2194–200.
36. Dempsey AR, Lloyd DG, Elliott BC, Steele JR, Munro BJ, Russo KA. The effect of technique change on knee loads during sidestep cutting. *Med Sci Sports Exerc* 2007;**39**:1765–73.
37. Villa FD, Tosarelli F, Ferrari R, et al. Systematic video analysis of anterior cruciate ligament injuries in professional male rugby players: Pattern, injury mechanism, and biomechanics in 57 consecutive cases. *Orthop J Sports Med* 2021;**9**:1–11. doi:10.1177/23259671211048182.
38. Meyer EG, Haut RC. Excessive compression of the human tibio-femoral joint causes ACL rupture. *J Biomech* 2005;**38**:2311–6.
39. Bates NA, Jaramillo MCM, Vargas M, et al. External loads associated with anterior cruciate ligament injuries increase the correlation between tibial slope and ligament strain during in vitro simulations of in *vivo* landings. *Clin Biomech (Bristol, Avon)* 2018;**61**:84–94.
40. Boden BP, Sheehan FT. Mechanism of non-contact ACL injury: OREF Clinical Research Award 2021. *J Orthop Res* 2022;**40**:531–40.
41. Koga H, Bahr R, Myklebust G, Engebretsen L, Grund T, Krosshaug T. Estimating anterior tibial translation from model-based image-matching of a noncontact anterior cruciate ligament injury in professional football: A case report. *Clin J Sport Med* 2011;**21**:271–4.
42. Shin CS, Chaudhari AM, Andriacchi TP. The influence of deceleration forces on ACL strain during single-leg landing: A simulation study. *J Biomech* 2007;**40**:1145–52.
43. Pflum MA, Shelburne KB, Torry MR, Decker MJ, Pandy MG. Model prediction of anterior cruciate ligament force during drop-landings. *Med Sci Sports Exerc* 2004;**36**:1949–58.
44. Ogasawara I, Shimokochi Y, Konda S, Mae T, Nakata K. Effect of rearfoot strikes on the hip and knee rotational kinetic chain during the early phase of cutting in female athletes. *Sports Med Open* 2021;**7**:75. doi:10.1186/s40798-021-00368-w.
45. Kristianslund E, Faul O, Bahr R, Myklebust G, Krosshaug T. Sidestep cutting technique and knee abduction loading: implications for ACL prevention exercises. *Br J Sport Med* 2014;**48**:779–83.
46. Sigward SM, Powers CM. The influence of gender on knee kinematics, kinetics and muscle activation patterns during side-step cutting. *Clin Biomech (Bristol, Avon)* 2006;**21**:41–8.

Please cite this article as: Issei Ogasawara et al., The deterministic condition for the ground reaction force acting point on the combined knee valgus and tibial internal rotation moments in early phase of cutting maneuvers in female athletes, Journal of Sport and Health Science (2024), https://doi.org/10.1016/j.jshs.2023.11.005